CrossMark

Photodegradation mechanisms of phenol in the photocatalytic process

Trinh Trung Tri Dang[1,2] · **S. T. T. Le**[1,2] ·
D. Channei[3] · **W. Khanitchaidecha**[1,2] ·
A. Nakaruk[4,5]

Abstract Investigating the photodegradation pathways of phenol, as well as the efficiency of photocatalysis by commercial TiO_2 is the main task in this present work. Commercial TiO_2 particles with the following characteristics: 96 % anatase, 4 % rutile, and 400 nm particles size were used as catalyst source. The photocatalytic process was carried out by mixing 100 ppm of phenol solution and 0.9 g/L of TiO_2 particles with magnetic stirrer under UV-C light with 210 nm wavelength. UV–Vis spectrophotometer and COD measurement were used to evaluate the efficiency of photocatalysis. On the other hand, the formed intermediate products during phenol photodegradation were identified by LC–MS, UV–Vis spectrophotometer, and photoluminescence techniques. The results indicated that phenol was removed completely after 24 h of UV-C irradiation. The absorbance peak of phenol slightly decreased during the first 16 h. However, the peak dramatically reduced and disappeared at 24 h of irradiation. This degradation mechanism also occurred similarly to the COD value. There were two phases in photocatalysis of phenol. In phase-I, phenol was decomposed to hydroxylated compounds such as catechol, benzoquinone, and complexes with two benzene rings. In the mineralization phase, hydroxylated compounds were mineralized strongly by hydroxyl radicals, hydrogen

✉ A. Nakaruk
auppathamn@nu.ac.th

1 Department of Civil Engineering, Faculty of Engineering, Naresuan University, Phitsanulok, Thailand

2 Centre of Excellence for Innovation and Technology for Water Treatment, Naresuan University, Phitsanulok, Thailand

3 Department of Chemistry, Faculty of Science, Naresuan University, Phitsanulok, Thailand

4 Department of Industrial Engineering, Faculty of Engineering, Naresuan University, Phitsanulok, Thailand

5 Center of Excellence for Environmental Health and Toxicology, Naresuan University, Phitsanulok, Thailand

radicals, and UV energy to form short-chain organic compounds such as formic acid, glycerol, and oxalic acid. Finally, hydrocarbon chains were broken easily and removed in the forms of carbon dioxide and water.

Introduction

Depletion of available water resources has received increasing attention globally owing to its critical role in socioeconomic development and human health. The scarcity of water resources has been attributed to the overuse of water as well as increasing pollution of water resources [1]. The pollution of industrial wastewater has become a major complicated issue owing to the increasing diversity of manufactured products and the associated variety in precursor chemicals that can disposed into the water resources [2]. Among the recalcitrant organic compounds, phenol is one of the most toxic, and is used widely in petrochemical, chemical, and pharmaceutical industries [3]. The presence of phenol in aqueous environments presents serious problems due to its toxicity, persistence in the environment, and bioaccumulation. In humans, contact with phenol can cause mouth sores, nausea, darkening of the urine, vomiting, and bloody diarrhea at varying concentrations [4]. In addition, oxidation and disinfection processes used to remove phenol can produce potentially carcinogenic compounds as chlorophenols [5]. Therefore, phenol removal by environmentally friendly is a major consideration for current research.

Recently, several technologies have been used for the efficient treatment of phenol, such as adsorption [6] and biological processes [7]. However, the quality of discharged wastewater has been subjected to increasingly stringent requirements to achieve greater environmental protection [8]. Further, technologies such as adsorption and coagulation can only transfer pollutants to other phases and cannot eliminate them completely [9]. Other methods such as sedimentation, filtration, chemical, and membrane technologies have high operating costs and/or generate secondary toxic pollutants in the treatment process; for example, the by-products from chlorination are mutagenic and carcinogenic compounds [10, 11]. Further, mentioned methods have not yet demonstrated sufficient effectiveness to meet the quality criteria and tend to generate non-biodegradable organic pollutants that appear in effluents with time [1]. Hence, alternative methods are required to solve these issues.

Recently, advanced oxidation processes (AOPs) are optimal alternative methods that have received much attention for removal of phenol. Although AOPs include different types of reaction systems, all of them follow the same principle, i.e., oxidation processes based on using hydroxyl radicals as the oxidizing species for destroying contaminants present in water [12]. Among AOPs, heterogeneous photocatalysis employing semiconductor catalysts has demonstrated efficiency in degrading organic compounds into readily biodegradable molecules that can be mineralized to carbon dioxide and water [11]. The basic principle of photocatalysis

is that the catalysts are excited by UV light and the resultant electrons and hole react with oxygen and/or water to produce highly oxidizing free radicals such as $OH^{.}$. Pollutants in water are then degraded by hydroxyl radicals to carbon dioxide and water forms. The type of semiconductor catalyst used has an important role in the photocatalytic process efficiency. TiO_2, ZnO, Fe_2O_3, CdS, GaP, and ZnS are semiconductor catalysts, which are often used in photocatalytic treatment [13]. Among these, titanium dioxide (TiO_2) has been used widely because of its non-photocorrosive and non-toxic nature, combine with its strong oxidation ability and high chemical stability [14]. In addition, TiO_2 has also shown to be the most active catalyst in previous studies [15, 16].

The effectiveness of photocatalysis for the decomposition of phenol has been investigated widely. Most research has suggested that phenol can be destroyed to carbon dioxide and water [17]. Further, some of the intermediate products formed during photodegradation of phenol have also been determined to be hydroquinone, resorcinol, and catechol (main by-products) along with other aliphatic and acidic compounds [18, 19]. Based on the by-products formed, general photodegradation pathways of phenol have been proposed by others [18, 20–23]. However, there is insufficient clarity in the intermediates formed during photocatalytic process until now, especially in using commercial TiO_2. Furthermore, a clear identification of intermediates, as well as photodegradation pathways of phenol is useful for investigating the degradation of its derivatives.

Therefore, the intention of this work was to investigate the efficiency of commercial photocatalytic TiO_2 for the degradation of phenol from water. The assessment of the degradation kinetics was done using a combination of UV–Vis spectrophotometer and chemical oxygen demand (COD) measurements. Moreover, the intermediate products formed during different steps in the photocatalytic degradation routes were determined by liquid chromatography–mass spectrometry (LC–MS).

Materials and methods

Photocatalytic experiments were carried out in a batch reactor with 50 mL of total solution volume. Commercial TiO_2 particles supplied from Sigma-Aldrich (reagent grade) were used as the photocatalyst. The characteristics of commercial TiO_2 particles were presented in a previous work [24], and the data are summarized briefly in the Table 1. The phenol solution was prepared by mixing 0.1 g of phenol

Table 1 Summary of the characteristics of commercial TiO_2 particle

Parameter	Value
Anatase (%)	95.97
Rutile (%)	4.03
Average particle size (nm)	400
Specific surface area (m^2/g)	9.73
Band gap (eV)	3.74

solid in 1 L of distilled water. TiO$_2$ (0.9 g/L) particles were added directly into 50 mL of phenol solution in a beaker. UV-C light with 215 nm wavelength was used in the cabinet of the reactor as the light source for irradiation of suspended solution. To avoid the settling of TiO$_2$ particles, the suspended solution was mixed by a magnetic stirrer at a rate of 100 rpm during the irradiation time.

The efficiency of phenol removal was evaluated by the decline in the height of absorbance peak at 270 nm [25] determined using UV–Vis double beam spectroscopy (*UV-6100*, Mapada). The COD value of the solution was measured using the COD analyser (*AL* 200CD, Aqualytic). The reaction kinetic in the photodegradation of phenol was also calculated by the Langmuir–Hinshelwood model [26] as shown in Eq. (1).

$$-\ln\left(\frac{C}{C_0}\right) = k_r k_{ad} t \qquad (1)$$

where k_r = intrinsic rate constant, k_{ad} = adsorption equilibrium constant, t = time.

In the present work, liquid chromatography–mass spectrometry (LC–MS) analysis was performed by using the Agilent 6540 Q-TOF LC–MS spectrometer (Agilent Technologies, Santa Clara, CA, USA) coupled with an Agilent 1260 infinity series HPLC system (Agilent, Waldron, Germany) to identify intermediate compounds during photodegradation of phenol. The HPLC system include a vacuum degasser with an auto-sampler and binary pump, a thermostatted column compartment. Additionally, this instrument was also connected to an electrospray ionization (ESI) source. The injection volume was 50 μL. In the HPLC, a mobile phase of 0.1 % formic acid in water and 50 % acetonitrile in methanol was employed in the gradient mode. The mass range was set at 50–300 *m/z*. All the acquisition and analysis of data were controlled by Mass Hunter software (Agilent Technologies). All of the samples were analyzed in negative mode to provide information for identification. In addition, photoluminescence analysis (*Fluoromax-4*, Horiba) was also used to confirm the LC–MS data, with 350 nm of the excitation wavelength.

Results and discussion

Figure 1 shows the degradation of phenol peak with irradiation time. The results indicated that the intensity of the phenol peak decreased gradually within the first 12 h of irradiation. However, there was a significant decrease in the peak after 16 h of irradiation, and the peak was absent after 24 h of irradiation. However, it should be noted that a red shift in the peak was apparent at ∼280 nm after just 2 h of irradiation, and this implies that phenol was degraded into intermediate compounds. In the meantime, the changes before 235 nm also showed the presence of these intermediates. Although the photocatalytic process was efficient in removing phenol using suspended TiO$_2$, the time for completion of degradation was ∼24 h. The slow rates of degradation are attributed to the highly stable benzene rings present in phenol, which are resistant to decomposition reactions.
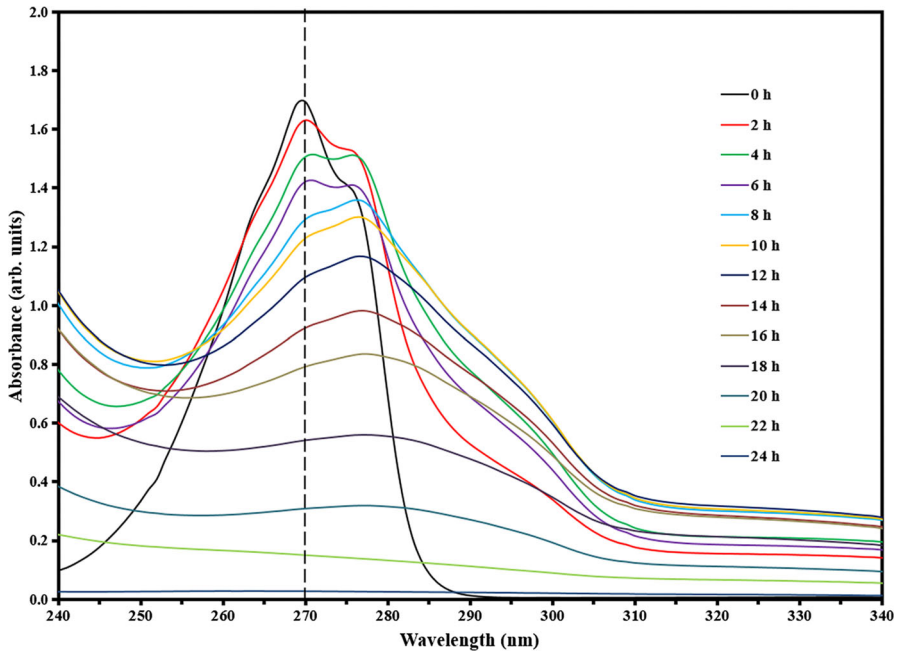
Fig. 1 Absorption spectra of solutions containing 100 ppm phenol after UVC irradiation for varying times

From the Fig. 1, it can be seen that a new peak at ~ 280 developed with increasing irradiation time, suggesting that intermediate products were formed during photocatalysis. Figure 2 shows the COD measurements, where there was a marginal decrease in the values during the first 12 h of irradiation. This suggests that there was only a limited transformation of phenol to CO_2, which was then lost from the solution. However, there was a dramatic decline in the COD value after 16 h of irradiation since hydrocarbon chains in the solution were mineralized into CO_2 and H_2O by the strong oxidative effects of hydroxyl and hydrogen radicals. In addition to the oxidizing radicals, UV energy was participated in the mineralization process by breaking weak bonds of hydrocarbon chains. This result has been proved by previous research [20, 27]. In theory, the bond energy of C–O (~ 350 kJ/mol), C–H (~ 400 kJ/mol), and H–O (~ 450 kJ/mol) are lower than the energy of UV light (~ 500 kJ/mol), thus a small part of the decomposition can be attributed to the sole effect of UV [20]. Although the effect of sole UV light in phenol degradation is not significant (Fig. 3) due to the resistant structure of benzene rings, other by-products having more simple and degradable structure can be degraded by UV light.

In addition to the photocatalysis, experiments with the absence of UV light and without catalysts in the presence of UV light were also carried out, as shown in Fig. 3. The results of these experiments indicated that phenol could not be decomposed without the catalysts or the UV light due to the highly stable benzene rings present in phenol.
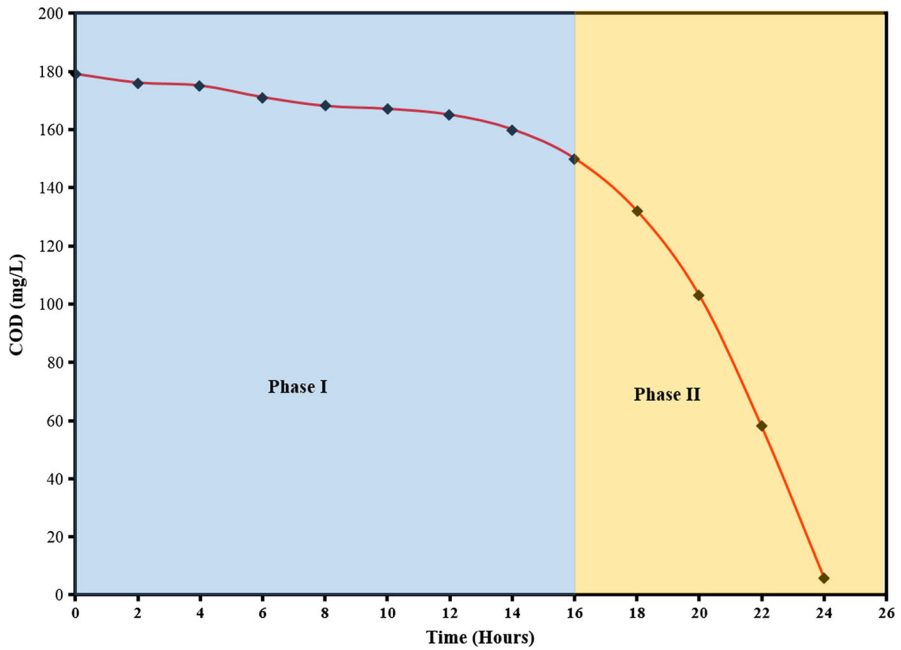
Fig. 2 Variation in COD values of the solution with UV-C irradiation time
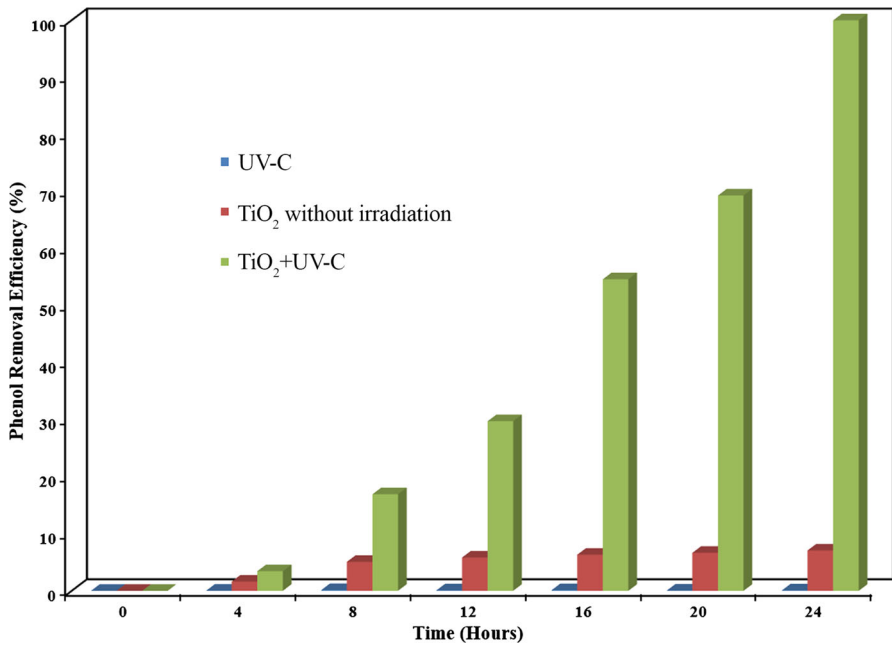
Fig. 3 Photodegradability of phenol in conditions without the catalyst and the UV light

The Langmuir–Hinshelwood model was used to describe the reaction kinetics of photocatalysis. The mineralization rate of phenol is illustrated by the slope of Eq. (1), as shown in Fig. 4. It is clear that phenol was mineralized at a quite low rate ($0.07 \ min^{-1}$) within the first 16 h of irradiation. However, the mineralization rate increased approximately three times after 16 h. This indicates that the mineralization rate of phenol increased proportionally with increasing irradiation time based on linear correlation ($R^2 = 0.99$) between the rate constant and irradiation times.

From these results, the photodegradation of phenol involves two stages, the first is the degradation of phenol to intermediate products, while the second involves mineralization of the intermediate compounds to carbon dioxide and water.

The results from LC–MS and photoluminescence analyses were used to determine the composition of the intermediate products. Several studies have presented that phenol shows resonance behaviour in water as illustrated in Fig. 5 [28–30].

Therefore, the $OH^.$ group released a proton easily to form phenoxide ions as shown in Fig. 6 [28]. The presence of these ions was seen through the LC–MS analysis of the solutions.

The release of a proton caused phenoxide ions in the initial phenol solution to show as a peak at 92.92 *m/z*, as presented in the below Fig. 7.

Hydroxyl radicals produced in the photocatalysis of oxidize phenoxide ions generated hydroxylated by-products. LC–MS showed a high intensity (2×10^5) of benzoquinone at 110 *m/z* after 4 h of irradiation, as shown in Fig. 8.
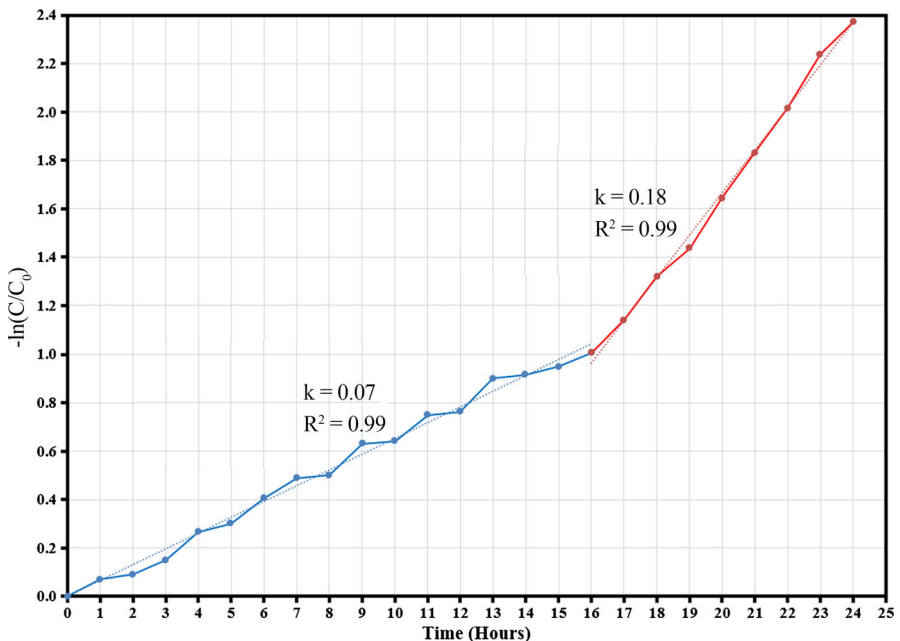
Fig. 4 Degradation kinetic of phenol in the photocatalytic process
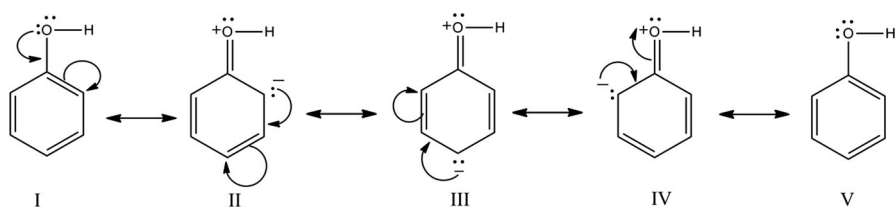
Fig. 5 Resonance states of phenol in water [25]
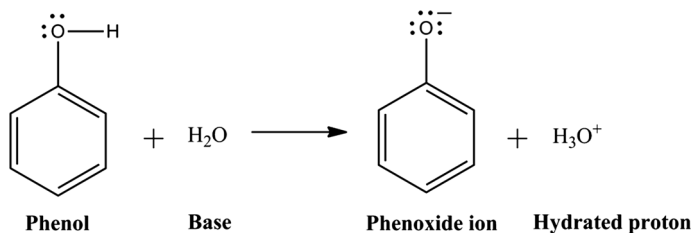
Fig. 6 Formation of phenoxide ions in water [28]
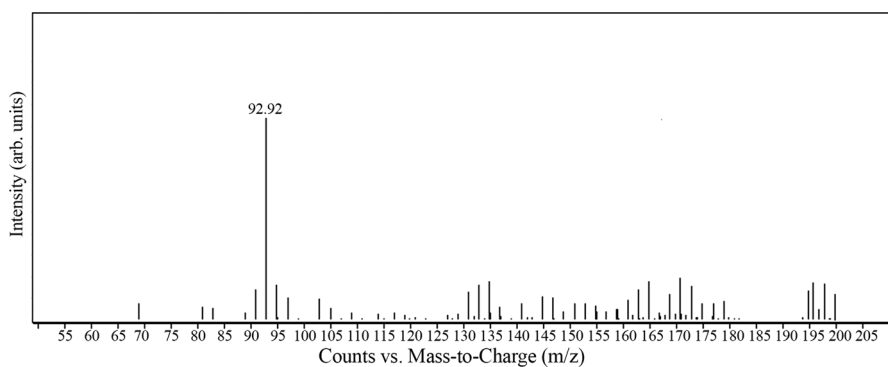
Fig. 7 Absorbance peak representing phenoxide ions determined using LC–MS
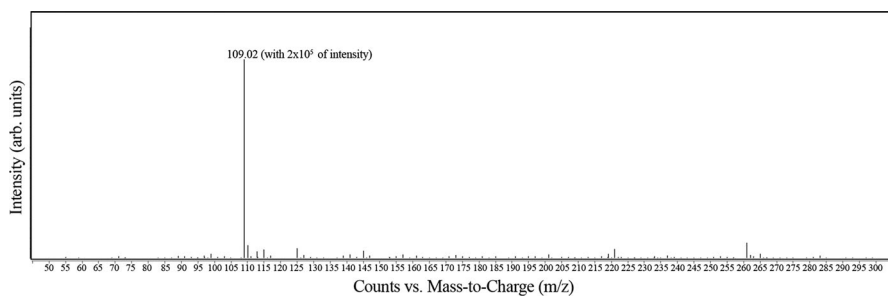
Fig. 8 Absorbance peak representing intermediates determined using from LC–MS after 4 h of irradiation

Furthermore, photoluminescence analysis (Fig. 9) also confirmed the presence of catechol and benzoquinone at ~450 nm wavelength [31]. No peak representing the phenol solution was found. However, catechol and benzoquinone were present after 3 h of irradiation and had the highest PL intensity. Continued photocatalysis resulted in degradation of these species with time leading to a lowering of the PL intensity.

Instability of these species (catechol and benzoquinone) transformed each other by giving and receiving electrons in a process called electrogenerated chemiluminescence (ECL), as shown in Fig. 10 [4]. In addition, the result also showed that the presence of these species decreased slightly over time, as seen in terms of reduction of PL peak.

On the other hand, more complex intermediates can form by combination of two phenoxide ions as shown in Fig. 11 [19]. This combination led to compounds with
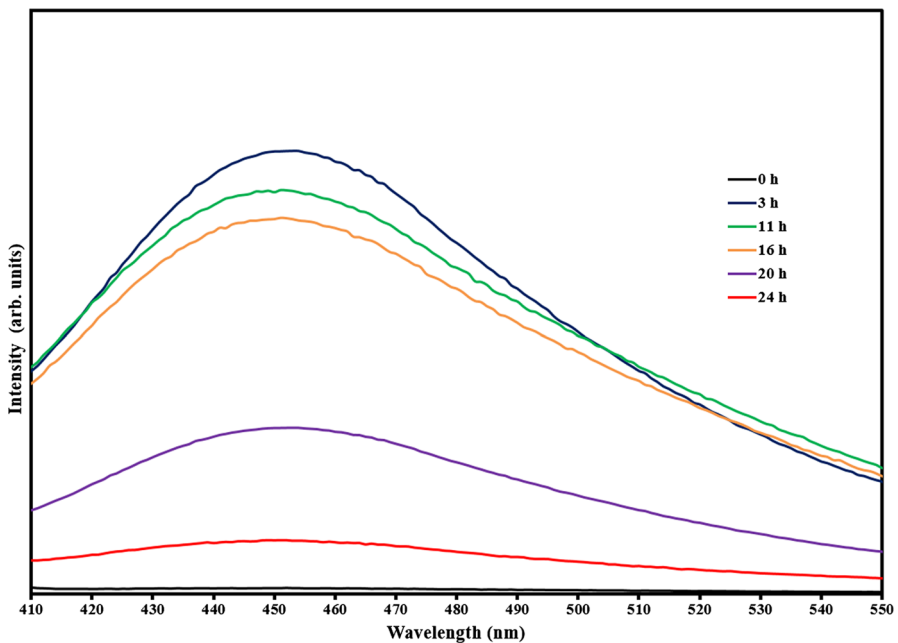
Fig. 9 Photoluminescence analysis data for phenol solution irradiated with UVC for varying times
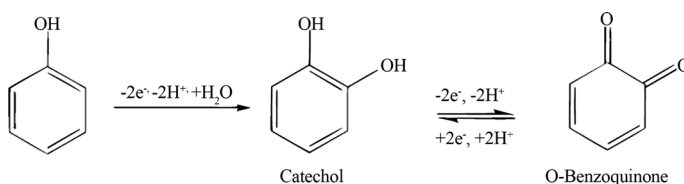
Fig. 10 Formation of catechol and benzoquinone from oxidation of phenol [4]

two benzene rings, such as 2-phenoxylcyclohexa-2,5-dienone, [1,1′-biphenyl]-4-ol or tectoquinone.

However, these complexes were easily broken down to back stabilizer compounds with an aromatic ring such as benzoquinone and catechol. As discussed
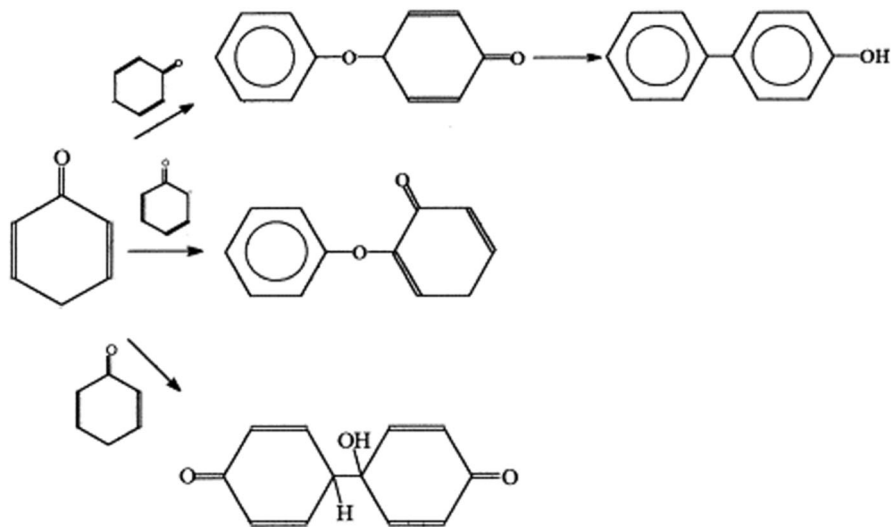
Fig. 11 Formation of complex intermediate products during photodegradation of phenol [19]

Ortho-dihydroquinone (Cathecol)   Ortho-benzoquinone   Hydroxyhydroquinone   Hydroxybenzoquinone
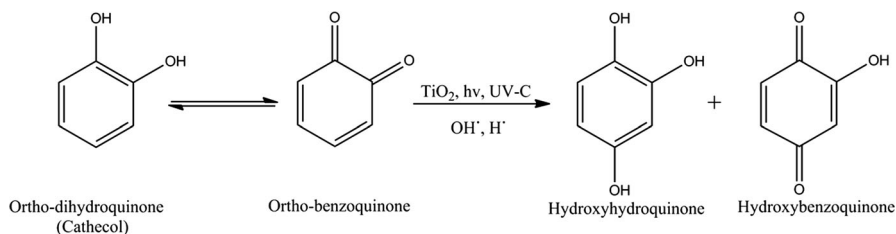
Fig. 12 Reaction representing the attack of OH radical on the benzene ring
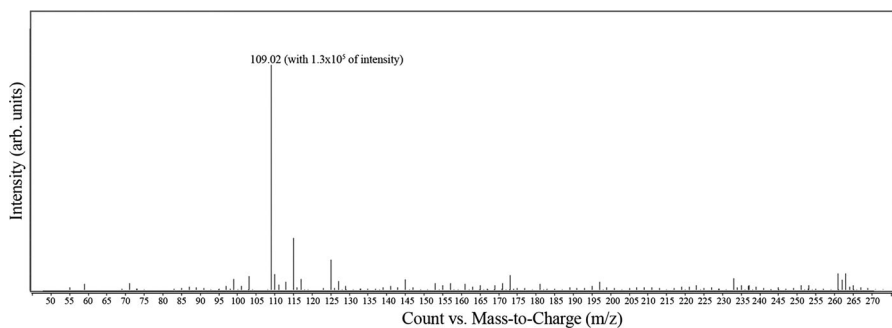
Fig. 13 Absorbance peak representing intermediates determined using LC–MS after 12 h of irradiation

Table 2 Products generated during photocatalytic degradation of phenol

Detection time (h)	Compound	Molecular weight (g/mol)	Chemical structure	Formula	References
0	Phenol	94	C_6H_6O		–
1	Catechol	110	$C_6H_6O_2$		[19, 21–23, 33–35]
1	Hydroquinone	110	$C_6H_6O_2$		[19, 21–23, 33–35]
1	Benzoquinone	108	$C_6H_4O_2$		[19, 21–23, 33–35]
1	2-Hydroxy methylanthraquinone	238	$C_{15}H_{10}O_3$		Present work
1	[1,1′-Biphenyl]-4,4′-ol	186	$C_{12}H_{10}O_2$		[19]
1	[1,1′-Bi(cyclohexane)-2,2′,5,5′-tetraene-4,4′-dione	186	$C_{12}H_{10}O_2$		Present work
1	2,2′,3-Trihydroxybiphenyl	202	$C_{12}H_{10}O_3$		Present work
1	2-Phenoxylcyclohexa-2,5-dienone	186	$C_{12}H_9O_2$		Present work
1	Oxoglutaric acid	146	$C_5H_6O_5$		Present work
1	Hydroxyl-benzoquinone	124	$C_6H_4O_3$		[21–23]
1	Butanol	72	C_4H_8O		Present work
1	Acrolein	56	C_3H_4O		Present work
4	1,2-Dihydroxyanthracene	240	$C_{14}H_8O_4$		[36]
4	Hydroxyl-hydroquinone	126	$C_6H_6O_3$		[19, 21–23, 35]
4	Maleic acid	116	$C_4H_4O_4$		[33]
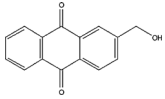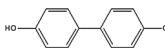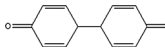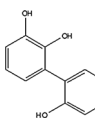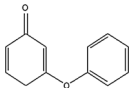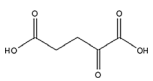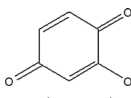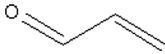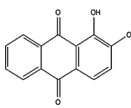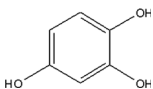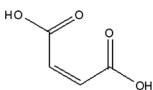
Table 2 continued

Detection time (h)	Compound	Molecular weight (g/mol)	Chemical structure	Formula	References
4	Oxalic acid	90	$C_2H_2O_4$		[33, 35]
8	Salicylic acid	138	$C_7H_6O_3$		[19, 35, 36]
8	Malonic acid	104	$C_3H_4O_4$		[33]
16	[1,1'-Biphenyl]-4-ol	171	$C_{12}H_{10}O$		Present work
16	Muconic acid	142	$C_6H_6O_4$		[33, 35]
16	Acetylenedicarboxylate	113	$C_4H_2O_4$		Present work
20	3-Butynoate	84	$C_4H_4O_2$		Present work
24	Glycerol	92	$C_3H_8O_3$		[35, 36]
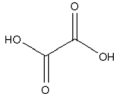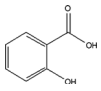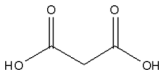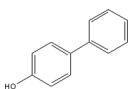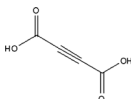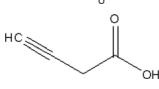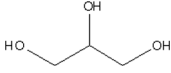
earlier, even though the benzene ring is a stable structure, the bond can potentially be weakened when OH radicals attack it, leading to the addition of one more OH group at the *ortho* or *para* positions. This reaction results in the formation of hydroxyl-hydroquinone and hydroxyl-benzoquinone from oxidation of catechol and benzoquinone, respectively, as shown in Fig. 12.

Two of these compounds were detected by LC–MS at 126 *m/z*, as seen in Fig. 13. After 12 h of irradiation, their absorbance peak increased gradually while the intensity of catechol (110 *m/z*) declined from $\sim 2 \times 10^5$ to $\sim 1.3 \times 10^5$ due to the formation of hydroxyl-hydroquinone and hydroxyl-benzoquinone.

As a result, a ring opening occurred, leading to the decomposition of phenolic compounds to short-chain organic compounds by hydroxyl and hydrogen radicals. This reaction accounts for the dramatic decrease in the COD value after 16 h of irradiation. Similar to previous research [32], glycerol, formic acid, and oxalic acid were major hydrocarbon chains formed in this process, as summarized in Table 2. Additionally, butanol, ethylene glycol and acetyl acid were also detected in this study. With the effects of UV irradiation, hydrocarbon chains were mineralized
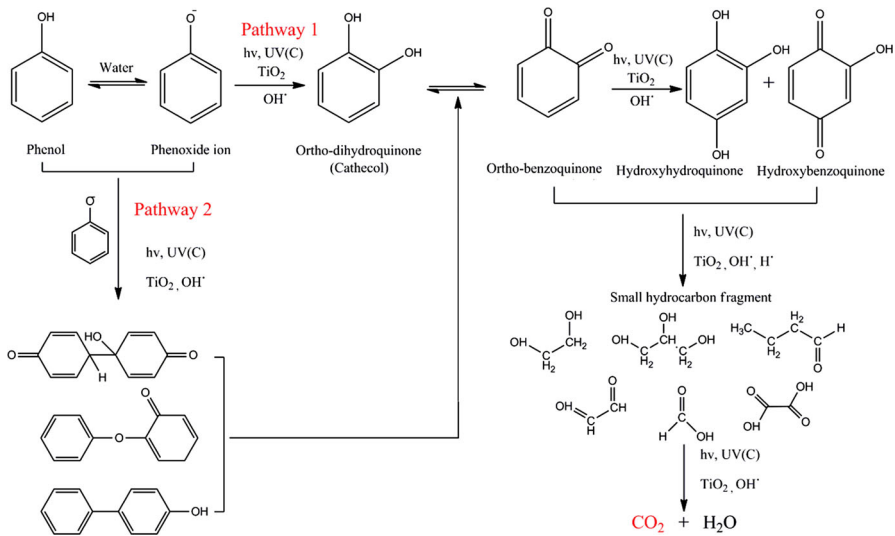
Fig. 14 A possible photodegradation scheme of phenol

completely to CO_2 and H_2O resulting in the significant decrease of COD value after 16 h.

From these results, the photocatalytic degradation of phenol involves the generation of intermediate compounds and a mineralization stage. The potential photodegradation pathway of phenol is shown in Fig. 14.

Conclusions

In the present work, photocatalysis using commercial TiO_2 particles was used to degrade completely the phenol present in water after 24 h of irradiation with UV-C. There was a steady decline in the amount of phenol within the first 16 h, after which there was drastic drop over the next 8 h of irradiation. This variation in the intensity of the phenol peak was reflected also in the COD values. The work revealed that there were two main stages of photodegration. In the first phase, phenol is degraded to complex hydroxylated by-products such as catechol, benzoquinone, biphenyl-4-ol, and short-chain compounds. In the mineralisation phase, these compounds are mineralised to CO_2 and H_2O. This stage involves a combined effect of radicals (hydroxyl and hydrogen) as well as UV, on decomposing simple hydrocarbons such as glycerol, formic acid, oxalic acid, butanol, ethylene glycol, and acetyl acid. To summarise, the photocatalytic process has been seen to be effective and efficient in removing phenol from water.

References

1. T. Teka, A. Reda, Int. J. Technol. Enhanc. Emerg. Eng. Res. **2**, 2347 (2014)
2. H. Eskandarloo, A. Badiei, C. Haug, Mater. Sci. Semicond. Process. **27**, 240 (2014)
3. I. Prabha, S. Lathasree, Mater. Sci. Semicond. Process. **26**, 603 (2014)
4. J. McCall, C. Alexander, M.M. Richter, Anal. Chem. **71**, 2523 (1999)
5. A. Hasanoglu, Desalination **309**, 171 (2013)
6. B.H. Hameed, A.A. Rahman, J. Hazard. Mater. **160**, 573 (2008)
7. A. Hussain, P. Kumar, I. Mehrotra, Bioresour. Technol. **99**, 8497 (2008)
8. M. Pera-Titus, V. Garcıia-Molina, M.A. Banos, J. Gimenez, S. Esplugas, Appl. Catal. B **47**, 219 (2004)
9. P.V.A. Padmanabhan, K.P. Sreekumar, T.K. Thiyagarajan, R.U. Satpute, K. Bhanumurthy, P. Sengupta, G.K. Dey, K.G.K. Warrier, Vacuum **80**, 1252 (2006)
10. U.I. Gaya, A.H. Abdullah, J. Photochem. Photobiol. C **9**, 1 (2008)
11. M.N. Chong, B. Jin, C.W.K. Chow, C. Saint, Water Res. **44**, 2997 (2010)
12. P. Navarro, J. Sarasa, D. Sierra, S. Esteban, I.L. Ovelleiro, Water Sci. Technol. **51**, 113 (2005)
13. M. Yasmina, K. Mourad, S.H. Mohammed, C. Khaoula, Energy Procedia **50**, 559 (2014)
14. K. Nakata, A. Fujishima, J. Photochem. Photobiol. C **13**, 169 (2012)
15. J. Zhou, Y. Zhang, X.S. Zhao, A.K. Ray, Ind. Eng. Chem. Res. **45**, 3503 (2006)
16. A. Thiruvenkatachari, S. Vigneswaran, I.S. Moon, Korean J. Chem. Eng. **25**, 64 (2008)
17. N. Barka, I. Bakas, S. Qourzal, A. Assabbane, Y. Ait-Ichou, Orient. J. Chem. **29**, 1055 (2013)
18. A. Sobczynski, L. Duczmal, W. Zmudzinski, Mol. Catal. A **213**, 225 (2004)
19. A.M. Peiro, A. Ayllon, J. Peral, X. Domenech, Appl. Catal. B **30**, 359 (2001)
20. Z. Guo, R. Ma, G. Li, Chem. Eng. **119**, 55 (2006)
21. A. Sclafani, L. Palmisano, M. Schiavello, J. Phys. Chem. **94**, 829 (1990)
22. G. Palmisano, M. Addamo, V. Augugliaro, T. Caronna, A. Di Paola, E.G. López, V. Loddo, G. Marcì, L. Palmisano, M. Schiavello, Catal. Today **122**, 118 (2007)
23. K. Okamoto, Y. Yamamoto, H. Tanaka, M. Tanaka, A. Itaya, Bull. Chem. Soc. Jpn **58**, 2015 (1985)
24. N. Yuangpho, S.T.T. Le, T. Treerujiraphapong, W. Khanitchaidecha, A. Nakaruk, Phys. E **67**, 18 (2015)
25. M.C. Neves, J.M.F. Nogueira, T. Trindade, M.H. Mendonca, M.I. Pereira, O.C. Monteiro, J. Photochem. Photobiol. A **204**, 168 (2009)
26. C.H. Chiou, C.Y. Wu, R.S. Juang, Chem. Eng. J. **139**, 322 (2008)
27. D. Chen, A.K. Ray, Appl. Catal. B **23**, 143 (1999)
28. V.P. Tyagi, *Essential chemistry XII* (Ratna Sagar P. Ltd., New Delhi, 2009)
29. P.S. Kalsi, *Organic reaction and their mechanism*, 2nd edn. (New age international, New Delhi, 2009)
30. P.W. Daniel, H.W. Arthur, *Pushing electron: a guide for students of organic chemistry*, 4th edn. (Cengage Learning, Boston, 2013)
31. G. Albarran, W. Boggess, V. Rassolov, R.H. Schuler, J. Phys. Chem. A **114**, 740 (2010)
32. L.G. Devi, K.E. Rajashekhar, Mol. Catal. A **334**, 65 (2011)
33. D. Duprez, F. Delanoe, J. Barbier Jr, P. Isnard, G. Blanchard, Catal. Today **29**, 317 (1996)
34. J. Moreira, B. Serrano, A. Ortiz, H. Lasa, Chem. Eng. Sci. **78**, 186 (2012)
35. E. Grabowska, J. Reszczynska, A. Zaleska, Water Res. **46**, 5453 (2012)
36. E.B. Azevedo, A.R. Torres, F.R. Aquino Neto, M. Dezotti, Braz. J. Chem. Eng. **26**, 75 (2009)